# Offline Assistance Optimization of a Soft Exosuit for Augmenting Ankle Power of Stroke Survivors During Walking

Christopher Siviy [ID], Jaehyun Bae, Lauren Baker, Franchino Porciuncula [ID], Teresa Baker, Terry D. Ellis, Louis N. Awad [ID], and Conor James Walsh [ID]

*Abstract*—Locomotor impairments afflict more than 80% of people poststroke. Our group has previously developed a unilateral ankle exosuit aimed at assisting the paretic ankle joint of stroke survivors during walking. While studies to date have shown promising biomechanical and physiological changes, there remains opportunity to better understand how changes in plantarflexion (PF) assistance profiles impact wearer response. In healthy populations, studies explicitly varying augmentation power have been informative about how exosuit users are sensitive to changes in PF assistance; however there are challenges in applying existing methods to a medical population where significantly higher gait variability and limited walking capacity exist. This letter details an offline assistance optimization scheme that uses pre-recorded biomechanics data to generate torque profiles designed to deliver either positive or negative augmentation power in PF while being less sensitive to stride-by-stride variability. Additionally, we describe an admittance-control strategy that can effectively deliver PF force with RMS error less than 10 N. A preliminary study on six people poststroke demonstrates that offline assistance optimization can successfully isolate positive and negative augmentation power. Moreover, we show that in people poststroke, positive augmentation power effected changes in total positive ankle power while delivering negative augmentation power had no effect on total negative ankle power.

*Index Terms*—Prosthetics and exoskeletons, rehabilitation robotics, wearable robots.

C. Siviy, J. Bae, L. Baker, F. Porciuncula, and C. J. Walsh are with the Harvard John A. Paulson School of Engineering and Applied Sciences and the Wyss Institute for Biologically Inspired Engineering, Cambridge, MA 02138 USA (e-mail: csiviy@g.harvard.edu; jhbae1107@gmail.com; lbaker@g.harvard.edu; fporciuncula@seas.harvard.edu; walsh@seas.harvard.edu).

T. Baker, T. D. Ellis, and L. N. Awad are with the Department of Physical Therapy and Athletic Training, Boston University and the Wyss Institute for Biologically Inspired Engineering, Boston, MA 02115 USA (e-mail: tcbaker@bu.edu; tellis@bu.edu; louawad@seas.harvard.edu).

## I. INTRODUCTION

THERE are seven million Americans living poststroke [1], more than 80% of whom experience locomotor impairments [2]. Often, people poststroke suffer from hemiparesis—the partial or complete paralysis of one side of the body—leading to gait that is typically slow, asymmetric, and inefficient [3]. Though deficits throughout the lower limb affect walking, ankle weakness is a primary contributor to impaired locomotor function.

In healthy walking, the ankle stores mechanical energy throughout early- and mid-stance (negative power), then releases that energy (positive power) during push-off in a "catapult mechanism" that serves two purposes: (1) propelling the body's center of mass forward and (2) initiating swing [4]. Impaired ankle function in people poststroke limits both, leading to decreased forward propulsion and poor foot clearance during swing. To stabilize the ankle, clinicians often prescribe ankle-foot orthoses (AFOs), which can return some walking function by supporting the ankle during stance and mitigating foot drop [5]. Because AFOs often feature rigid construction, they can limit the ankle's ability to push off [6] and lower muscle activation in dorsiflexors [7]. Therefore, researchers have recently become interested in lightweight wearable robotic devices that may improve upon AFOs and other passive devices in people poststroke [8]–[11]. Such devices have demonstrated promising outcomes, reducing gait compensations [10] and increasing push-off [8], [10], [11]. Our group has developed soft wearable robots called exosuits that can deliver mechanical power to the paretic ankle via functional textiles and Bowden cables connected to proximally-worn actuators [10], [11]. While soft exosuits have been shown to reduce the metabolic cost of walking, decrease circumduction, and increase paretic propulsion, [10] noted that individual participants may have different responses to changes in plantarflexion (PF) actuation timing. It is unclear if there is any systematic relationship between changes in PF assistance and ankle biomechanics.

Work in healthy populations has shown that the amount of positive augmentation power—the positive power that a wearable device delivers to the ankle—can significantly impact the effect of exoskeletons in terms of metabolic benefit [12], [13] and biomechanics [14]. In fact, an "augmentation factor" based primarily on positive augmentation power turns out to describe

the metabolic benefit of wearable devices with considerable accuracy ($R^2 = 0.98$) [13].

While the Achilles tendon is able to efficiently store mechanical energy, energy is still required to contract the muscle either isometrically or eccentrically [4]. Augmenting negative power in parallel with the muscle could therefore provide metabolic benefits. Limited prior investigation of negative power augmentation hints that this may be true: a completely passive exoskeleton [15] showed metabolic reductions by applying net-zero work, and a study described in [16] found a trend relationship between increasing negative power (while holding positive augmentation power constant) and metabolic reduction. Poor muscle coordination and weakness in people poststroke could inflate the cost of biological negative power production, leading to deficits—metabolic and otherwise—that negative power augmentation could alleviate.

Beyond metabolic benefits, varying power assistance has been valuable in studying how wearable exoskeletons affect ankle kinematics and kinetics. Quinlivan *et al.* [14] indicated that as net augmentation power increased in healthy individuals, so did total ankle power (combined biological power—generated by the body—and augmentation power). The effect was not accompanied by a decrease in biological power. An increase in total positive ankle power was accompanied by a decrease in peak dorsiflexion (DF) angle during stance, possibly decreasing the length of PF muscle-tendon units, thereby limiting the Achilles tendon's ability to store energy during early stance.

Still, to our knowledge no studies to date have explicitly varied delivered work or power in people poststroke. In fact, control strategies in the literature tend to deliver both negative and positive augmentation power [11], limiting researchers' ability to understand the relative benefits of either. Medical applications are a more recent focus for the field, and due to variability in walking after a stroke, it is unlikely that strategies that have successfully isolated either positive or negative augmentation power in healthy populations will work in people poststroke.

Fig. 1 demonstrates these challenges with foot-mounted gyroscope data from a healthy individual (data published in [16]) compared to similar data from a person poststroke (from the present study). Both [16] and [17] relied on the point at which ankle angular velocity switches signs to trigger the onset of assistance; their soft exosuit delivered only PF torques, so any assistance delivered after the event marked in Fig. 1(C) delivered positive augmentation power. While both sets of data were recorded on a treadmill at comfortable walking speed, there is notably increased variability in the person poststroke (Fig. 1(B) and (C)).

Other methods of automatically tuning assistive torque profiles are promising, but are similarly unproven in clinical populations. There is interest in using human-in-the-loop (HIL) methods—a recently-developed technique that uses real-time recordings of the metabolic cost of walking and adapts a force profile according to some optimization strategy—to achieve something similar [18]. However, the variability exhibited in Fig. 1 may make it difficult to converge on a single "optimal" profile. Further, extended experiment times required for HIL experiments—often stretching into hours—are prohibitive for
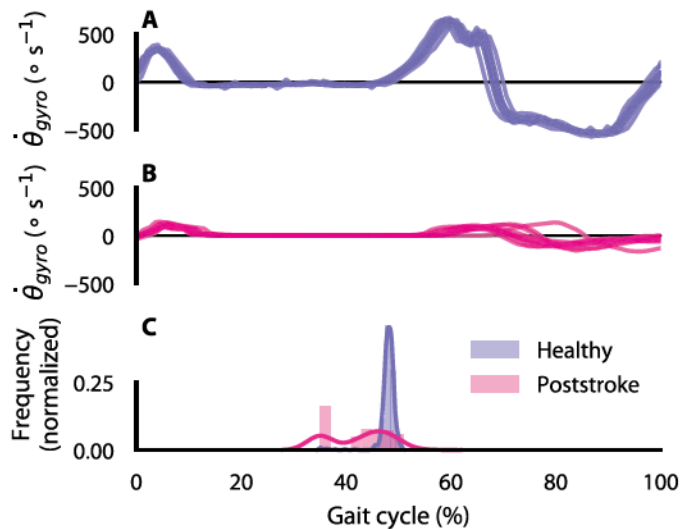
Fig. 1. (A) Foot-mounted gyroscope data ($\dot{\theta}_{gyro}$) from a representative healthy individual [16]. (B) Foot-mounted gyroscope data from a representative poststroke participant. (C) Histograms of the estimated ankle-velocity zero crossing for both the healthy individual and the person poststroke. Lee *et al.* [17] uses this zero crossing to trigger force onset. Both data were collected at the participant's comfortable walking speed. Ankle angular velocity was estimated using a foot-mounted gyroscope noting that shank angular velocity is negligible compared to foot angular velocity during the period of interest.

people poststroke. Possibly, a method partway between manual tuning and HIL optimization could incorporate biological data while being less susceptible to variability and poor ankle angular velocity estimation.

Accordingly, we propose an offline assistance optimization approach that uses pre-recorded kinematics to optimize a best-guess assistance profile meant to apply either positive or negative power. Implicitly, this carries the assumption that kinematics do not change when assistance is applied, or across multiple days. From our past work applying assistance at the paretic ankle with a soft exosuit [10], [11], we do see some changes in kinematics; though these changes have been greater for DF compared to PF. We hypothesize that using biological data will inform the design of assistive profiles that deliver mostly positive or negative augmentation power while rejecting the other. Further, optimizing assistance offline enables more sophisticated optimization algorithms than currently-available hardware allows; it is possible to optimize the entire force profile rather than changing a few discrete knot points (as in [18]) or reacting to events as they happen (as in [16], [17]). Optimizing the entire assistance trajectory also means that varying just a few physically-interpretable hyperparameters (e.g. penalties on either estimated positive or negative augmentation power) can yield vastly different torque profiles without manual input from an engineer.

## II. Soft Exosuit for Assisting Walking Poststroke

The soft exosuit comprises two sets of components: functional apparel that anchor forces to the body and a torso-mounted actuation system containing motors that generate assistive torques. Total system mass (Table I) is 4932 g, with 4471 g worn

**TABLE I**
**SOFT EXOSUIT COMPONENTS AND THEIR MASS**

| Component | Mass (g) |
|---|---|
| Actuator and cables* | 3392.5 |
| Calf wrap and sensors | 352.3 |
| Battery | 1079.4 |
| Insole | 108.0 |
| **Total** | **4932.2** |

*Note that the actuator used here is approximately 1 kg heavier than that published in [11].

proximally on the torso to mitigate the impact of energetically costly distal mass.

### A. Textile Components and Actuation System

For a detailed description of the soft exosuit's textile components, see [11]. Briefly, the soft exosuit consists of a custom-fabricated waist belt and calf wrap, plus an insole inserted into the shoe. The insole features textile components that connect to the distal ends of inner Bowden cables, with the outer Bowden cable sheath anchored at the calf wrap. Therefore, retracting the inner Bowden cable generates an assistive torque purely about the ankle.

At typical loads during walking, the actuation hardware published in [11] could retract cable at a maximum velocity of $550 \text{ mms}^{-1}$. Pilot testing revealed that this velocity limit was too low to apply the range of desired torque profiles for the present study. Therefore, the present study uses actuation hardware adapted from [19] with modifications to better mount to the body and attach to both textile and sensing components on the soft exosuit. The updated actuation system is capable of retracting cable at a maximum velocity of $800 \text{ mms}^{-1}$.

### B. Control System

Prior work in soft exosuits for poststroke paretic ankle assistance used a force-based position controller that adapts Bowden cable position based on selected force measurements. This approach measures cable force at key points during the current stride—peak force, timing of force onset, and timing of force offset—and updates position commands for the next stride accordingly. While force-based position controllers can deliver accurate peak torque, onset time, and offset time, they do not allow an offline trajectory generator to prescribe an entire force profile. Therefore, we developed a new force controller using an admittance control strategy inspired by previous work providing assistance at the hip [20] (Fig. 2). An admittance control approach allows us to command a complete force profile, allowing an experiment that can explicitly vary augmentation power, which was not possible using the control strategy from [11].

Similar to our previous controller [11], this controller consists of two nested control loops. First, the inner layer runs closed-loop control on motor velocity for the actuation system to track the desired cable velocity trajectories generated by the outer layer (see [11] for further detail). The outer layer includes two feedforward compensators that account for the changes in Bowden cable position induced by joint motions (joint motion

compensator) and the cable force generation due to the deformation of exosuit worn on the human body (human-exosuit stiffness). Residual force error is then compensated through a feedback admittance controller that generates cable velocity command based on force error measurements.

The joint motion compensator generates desired cable velocity ($v_{ank}$) to compensate ankle rotational motion by estimating sagittal plane ankle velocity with inertial measurement units (IMUs) attached to the paretic shank and foot:

$$v_{ank} = r \left( \dot{\theta}_{shank} - \dot{\theta}_{shoe} \right) \tag{1}$$

where $\dot{\theta}_{shank}$ and $\dot{\theta}_{shoe}$ are the angular velocity of the shank and foot and $r$ is a moment arm between the cable line of action and the ankle joint center (estimated as 7.4 cm during pilot testing). Human-exosuit stiffness was modeled according to

$$x_{exo} = C_1 \log \left( C_2 F_{exo} + 1 \right) \tag{2}$$

meaning

$$v_{exo} = \frac{C_1 C_2}{C_2 F_{exo} + 1} \dot{F}_{exo} \tag{3}$$

where $x_{exo}$ is PF cable position, $v_{exo}$ is Bowden cable velocity, and $F_{exo}$ is desired force. Constants $C_1$ and $C_2$ were calculated using least-squares regression on empirical data of Bowden cable position and force (see Section IV-A for more detail on controller tuning).

Finally, the admittance controller generates desired cable velocity $v_{fb}$ based on residual force error that was not compensated for by the feedforward blocks as

$$v_{fb} = \frac{1}{M_v s + C_v} F_{err} \tag{4}$$

where $v_{fb}$ is the desired cable velocity in the Laplace domain and $F_{err}$ is the difference between commanded and measured force in the Laplace domain. Tuning parameters $M_v$ and $C_v$ are virtual inertia and damping constants, respectively. The final velocity command input to the inner control layer was calculated as the sum of $v_{ank}$, $v_{exo}$, and $v_{fb}$. Preliminary validation of this controller on a single healthy individual demonstrated RMS error less than 6 N, which is similar to error reported in [20].

### III. OFFLINE ASSISTANCE OPTIMIZATION

We investigated an offline assistance optimization scheme for PF assistance only, leaving DF assistance under position control as in previous work [10], [11]. Not varying DF assistance preserved similarity to [14], which was conducted in healthy individuals and did not deliver DF assistance.

First, PF cable force $F_{PF}$ was discretized into 100 points evenly distributed across the gait cycle. Then estimated positive augmentation power $\hat{P}_{aug}^+$ and negative augmentation power $\hat{P}_{aug}^-$ were calculated as

$$\hat{P}_{aug}^+ = F_{PF} \, r \, \dot{\theta}_{ank}^+ \tag{5}$$

$$\hat{P}_{aug}^- = F_{PF} \, r \, \dot{\theta}_{ank}^- \tag{6}$$

where $\dot{\theta}_{ank}^+$ is any ankle angular velocity in the positive (i.e. PF) direction and $\dot{\theta}_{ank}^-$ is any ankle angular velocity in the negative
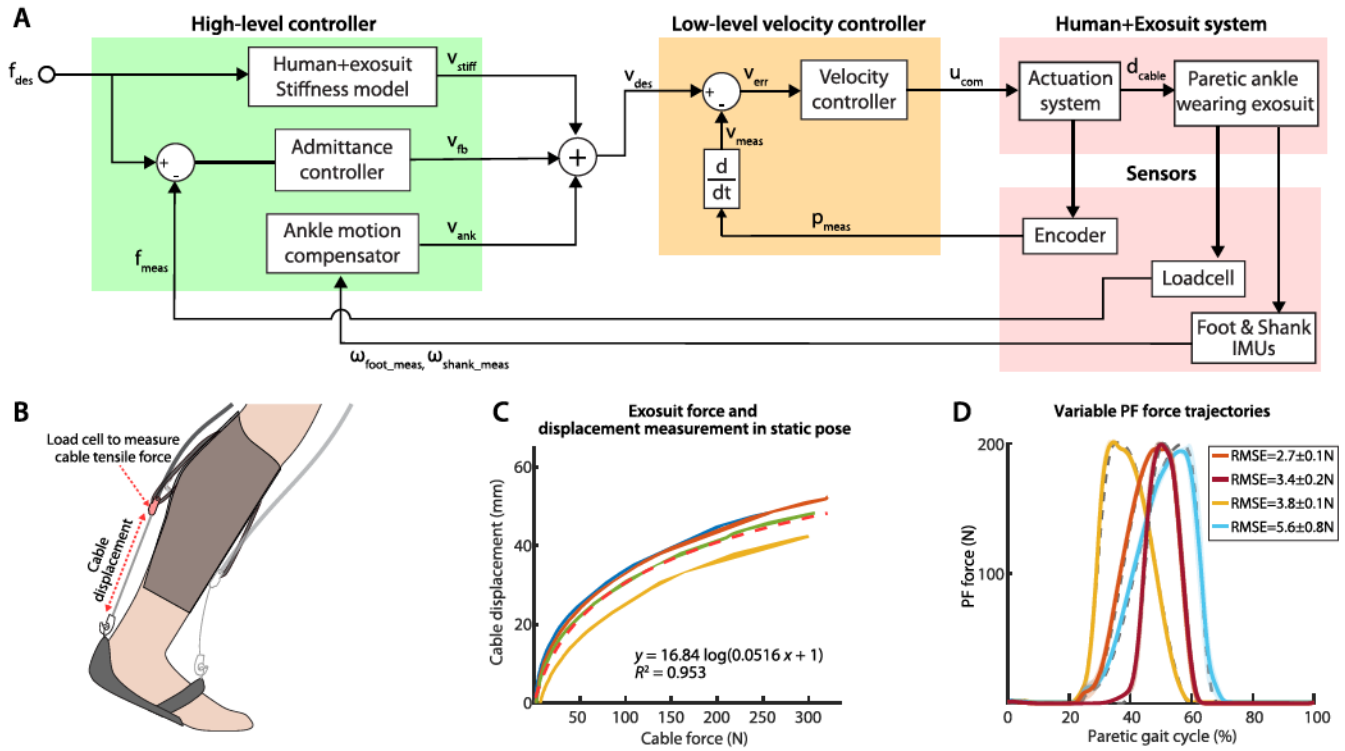
Fig. 2.   (A) Diagram of the admittance controller. (B) Illustration of the static pose to measure cable force in different cable displacements for human+exosuit stiffness modeling. (C) Relationships of cable force and displacement measurements from four different healthy individuals (solid lines, each color a different individual) and their logarithmic fit (dotted line). (D) Effect of changing PF onset timing and PF peak timing on a single healthy individual.

(i.e. DF) direction, both from pre-recorded motion capture data. PF force was then calculated according to

$$F_{PF} = \arg\min_{F_{PF}} \left[ -\alpha_+ \sum_{\text{stride}} \hat{P}_{aug}^+ + \alpha_- \sum_{\text{stride}} \hat{P}_{aug}^- \right.$$

$$\left. + \alpha_F \sum_{\text{stride}} \ddot{F}_{PF}^2 \right] \quad (7)$$

$$\text{subject to} \quad \max\left[F_{PF}\right] \le F_{max}$$

$$\text{Onset after } t_{start}$$

$$\text{Offset before } t_{end}$$

where $\alpha_+$ is a reward on estimated positive augmentation power, $\alpha_-$ is a penalty on estimated negative augmentation power, and $\alpha_F$ is a penalty on the second derivative of $F_{PF}$. Accordingly, when $\alpha_+, \alpha_- > 0$, $F_{PF}$ will prefer positive augmentation power. When $\alpha_+, \alpha_- < 0$, $F_{PF}$ will prefer negative augmentation power. The third term is a smoothing factor that ensures each optimized trajectory is physically achievable; otherwise $F_{PF}$ would simply follow $F_{max} \operatorname{sign} \theta$. Limits $t_{start}$ and $t_{end}$ were set such that $t_{start}$ was at 10% of the period between non-paretic foot contact and paretic foot lift, and $t_{end}$ was 2.5% of the gait cycle after paretic foot lift.

Fig. 3 varies $\alpha_+$ and $\alpha_-$ with $\alpha_F$ held constant so only $\alpha_+/\alpha_-$ determines the profile's shape. Though illustrative of our method's ability to dramatically vary force profiles by changing just $\alpha_+$ and $\alpha_-$, it is important to note that allowing $\alpha_F$ to
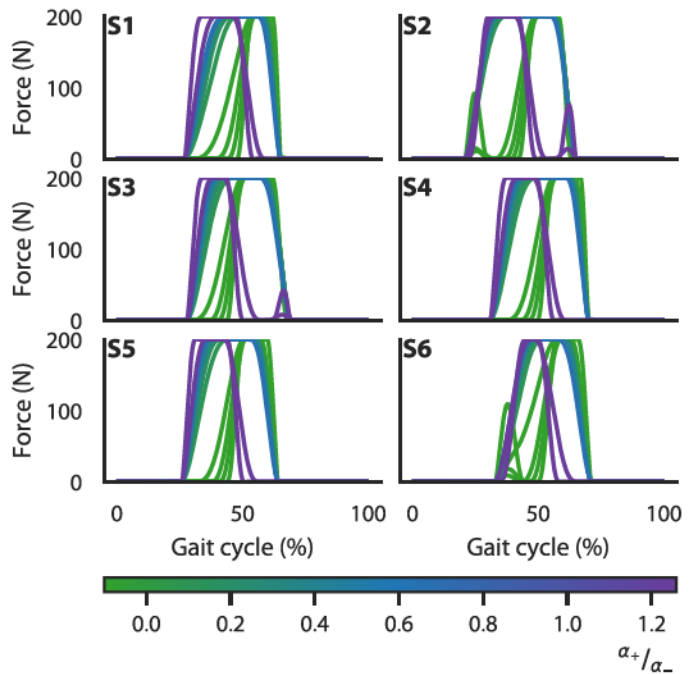


Fig. 3.   Effect of varying the ratio between $\alpha_+$ and $\alpha_-$ on optimized force profiles for six participants using data collected in the present study. These data show the effect of varying $\alpha_+$ and $\alpha_-$ while holding $\alpha_F$ constant at $\alpha_F = 1$.

vary would change these trajectories substantially. In general, profiles biased toward positive power tend to be later in the gait cycle, when PF velocity is the highest and profiles biased toward
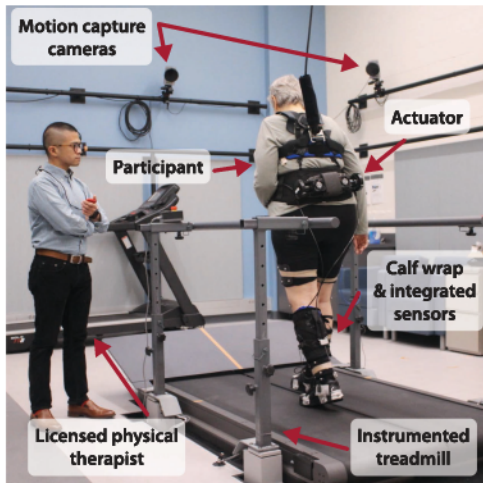
Fig. 4. Setup for experimental validation. Study participants walked on a treadmill while wearing the exosuit.

negative power tend to be earlier in stance (see Fig. 8 for plots of typical ankle angular velocity).

## IV. EXPERIMENT

### A. Control System Tuning

The admittance controller described in Section II-B was initially tuned on a single healthy individual walking on a treadmill at multiple speeds ranging from 0.5 ms$^{-1}$ to 1.5 ms$^{-1}$ and used for the following experimental studies with poststroke participants (see Section IV-B). First, the human-exosuit stiffness model in Fig. 2(A) was approximated based on the exosuit force and displacement collected from three healthy individuals. These healthy individuals stood in a static pose while wearing the exosuit. Participants stood such that the limb wearing the exosuit approximated the leg's orientation during push-off (see Fig. 2(B)(C)). Second, $M_v$ and $C_v$ in (4) were iteratively tuned to achieve sufficiently low RMSE for various PF force commands (Fig. 2(D)) while a healthy individual was walking on a treadmill. Note that the controller was not re-tuned for individual poststroke participants or adapted for changes in walking speed and desired peak force.

### B. Experimental Validation

To evaluate whether offline assistance optimization can successfully deliver isolated positive and negative augmentation power, we conducted an experimental validation with six chronic stroke participants (participant characteristics are in Table II). Participants walked on an instrumented split-belt treadmill (Bertec, USA; 2000 Hz) while ten motion capture cameras (Oqus, Qualisys, Sweden; 200 Hz) recorded full-body kinematics. Joint angles were calculated via direct kinematics and joint moments and powers were calculated using inverse dynamics (Visual 3D, C-Motion, USA). Fig. 4 shows the experimental setup. First, participants walked unassisted on the treadmill for a brief one- to two-minute bout to determine their comfortable walking speed. Next, participants walked at their

### TABLE II
### PARTICIPANT CHARACTERISTICS

| Participant | Age (yr) | Body mass (kg) | Years poststroke | Walking speed (ms$^{-1}$) |
|---|---|---|---|---|
| S1 | 33 | 57.3 | 11 | 0.75 |
| S2 | 34 | 91.5 | 6 | 1.30 |
| S3 | 54 | 84.5 | 4 | 0.35 |
| S4 | 77 | 101.8 | 8 | 0.60 |
| S5 | 49 | 43.9 | 5 | 0.55 |
| S6 | 62 | 66.3 | 3 | 0.40 |

comfortable walking speed for four three-minute trials: (1) a condition where (7) was tuned to apply negative augmentation power ($P^-$); (2) a condition where (7) was tuned to apply positive augmentation power ($P^+$); (3) a condition using the force-based position controller described in [11] ($P^\pm$); and (4) a condition not wearing the exosuit at all (*NOST*). Medical clearance and written informed consent forms approved by the Harvard University Human Subjects Review Board were received from all participants. For all participants, we used a reference trajectory for $\dot{\theta}_{ank}$, but updated $t_{start}$ and $t_{end}$ on an individual basis using overground data collected during a prior five-minute condition not wearing the exosuit.

In $P^-$ the parameters for (7) were set as $\alpha_+ = -0.733$, $\alpha_- = -1$, and $\alpha_F = 0.733$, and in $P^+$ $\alpha_+ = 1$, $\alpha_- = 0.733$, and $\alpha_F = 0.733$—values determined as feasible during initial pilot testing. Between ankle angular velocity and temporal metrics such as foot lift and initial contact, the latter is much less time-consuming to collect, so this approach allowed some level of individualization without requiring costly motion capture data from each participant. Moreover, Fig. 3 shows that when optimizing for either mostly positive or mostly negative power, (7) is less sensitive to individual ankle angular velocity profiles than cases that apply a mixture of negative and positive augmentation power. In all conditions, peak force was set at 25% body weight, as in [10], [11], [21]. To preserve the relative weight of $\alpha_F$ across all participants, force profiles were first calculated using a peak force of 200 N, then scaled to 25% body weight. Augmentation power was calculated as

$$P_{aug} = r \, F_{PF} \dot{\theta}_{ank}. \tag{8}$$

Statistical significance was assessed using one-way ANOVA and pairwise comparisons used Tukey's Honestly Significant Difference test, with significance set at $p < 0.05$. Correlations between total ankle power and augmentation power were determined using Pearson's correlation. We hypothesized that the offline assistance optimization scheme above would selectively deliver either positive or negative net augmentation power and that the force-based position controller from [11] would deliver a mixture of positive and negative augmentation power. Biomechanically, we hypothesized that the biological ankle would respond differently to positive and negative power augmentation and that changes in ankle angular velocity, if any, would not negatively influence the desired augmentation power delivery.
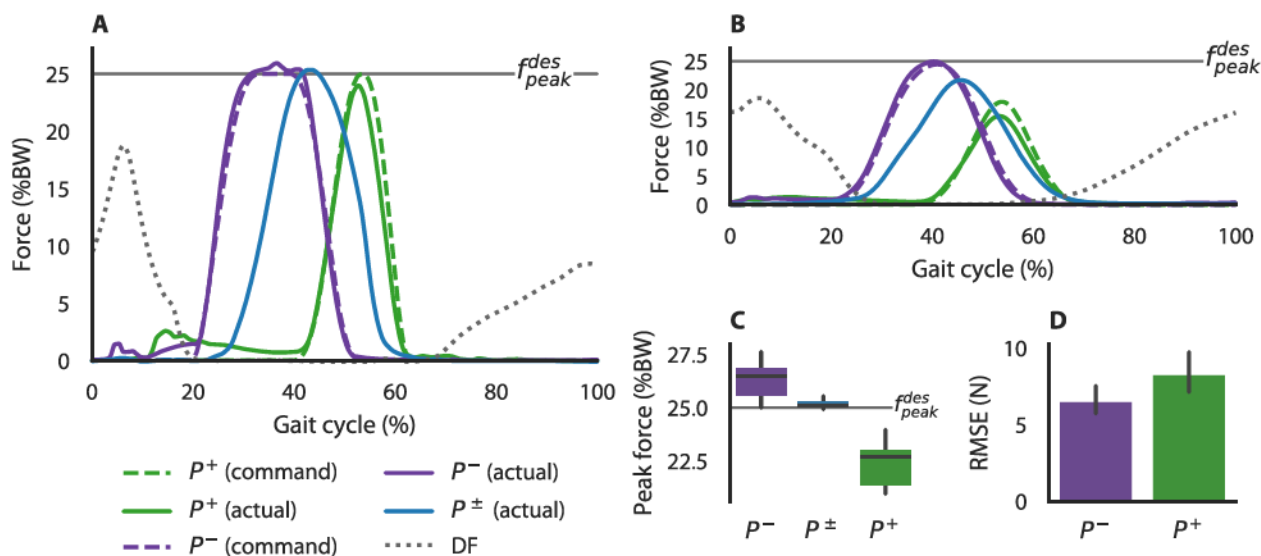
Fig. 5. (A) Representative commanded and measured torque profiles from one participant. (B) Mean force profile across all participants. (C) Box plots of peak force for each condition across all participants. (D) Mean RMSE force profile across all participants for the $P^+$ and $P^-$ conditions, the two that used admittance control.
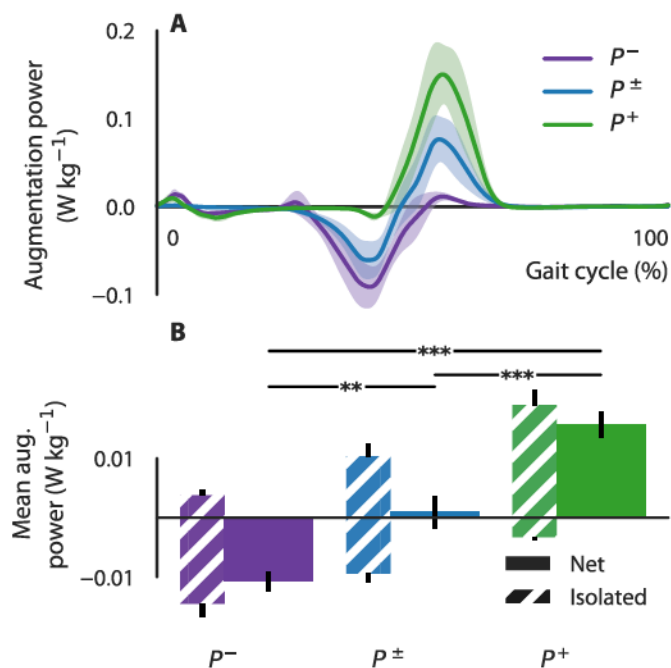


Fig. 6. (A) Average augmentation power across all participants. Shaded regions indicate standard error of the mean. (B) Mean augmentation power (net work divided by stride time) across all participants. Lighter hatched bars show mean positive power *only* and negative power *only*, while darker bars show net power. Asterisks denote significance using Tukey's HSD test (**: $p < 0.01$, ***: $p < 0.001$).

## V. RESULTS AND DISCUSSION

### A. Controller Performance

Differences between commanded and actual force profiles were small, as illustrated in Fig. 5. Mean RMSE across all participants during the period of PF assistance was $8.29 \pm 1.75$ N in $P^+$ and $6.55 \pm 1.22$ N in $P^-$ (Fig. 5(D)), the two conditions

that used force control. Peak PF force tracking, however, did differ among the three active conditions tested. Designed to track a specified peak PF, peak force error in $P^\pm$ was minimal. Peak force tracking was better in $P^-$ than $P^+$, but $P^-$ on average overshot the intended force profile while $P^+$ tended to undershoot (Fig. 5(C)). Fig. 5(A) shows representative assistance for a single stride; as assistance profiles in $P^+$ typically generated high force over a small amount of time, averaging across all participants in Fig. 5(B) makes $P^+$ assistance appear artificially low.

### B. Augmentation Power

Mean net augmentation power was defined as the integral of augmentation power divided by stride time; mean positive or negative augmentation power ("isolated" augmentation power) was defined as the integral of either positive or negative augmentation power divided by stride time. Offline assistance optimization successfully delivered either net positive augmentation power or net negative augmentation power as desired (Fig. 6), with a statistically significantly different amount of mean net augmentation power among all conditions tested ($P^-$: $-1.07 \pm 0.39 \times 10^{-02}$ Wkg$^{-1}$; $P^\pm$: $09.56 \pm 66.10 \times 10^{-04}$ Wkg$^{-1}$; $P^+$: $1.57 \pm 0.54 \times 10^{-2}$ Wkg$^{-1}$). Each of $P^+$ and $P^-$ was also able to effectively isolate the desired type of augmentation power, with $P^-$ delivering $3.77 \pm 2.13 \times 10^{-3}$ Wkg$^{-1}$ of positive augmentation power compared to $1.44 \pm 0.55 \times 10^{-2}$ Wkg$^{-1}$ of negative augmentation power, and $P^+$ delivering $-3.27 \pm 1.18 \times 10^{-3}$ Wkg$^{-1}$ of negative augmentation power compared to $18.90 \pm 05.94 \times 10^{-2}$ Wkg$^{-1}$ of positive augmentation power.

### C. Effects on Biological Ankle

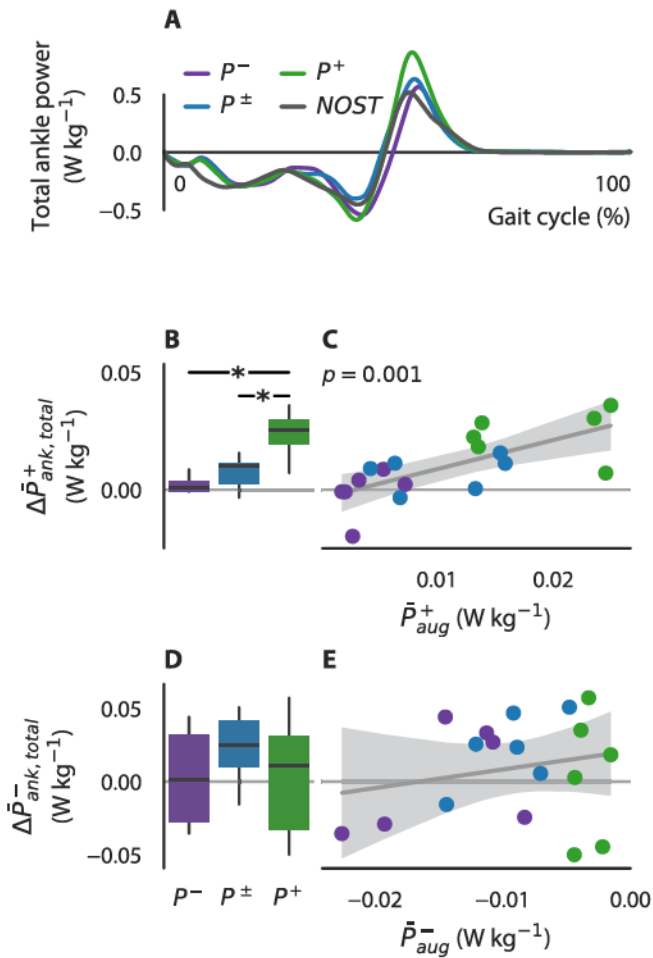We examined the biomechanical impact of positive and negative augmentation power in two ways. First, we tested the

Fig. 7. (A) Average total ankle power across all participants. (B) Change in mean positive power ($\Delta \bar{P}^+_{ank,total}$) for each condition. (C) Correlation between positive augmentation power and positive total ankle power ($y = -0.0037 + 1.2x$, $R^2 = 0.494$, $p = 0.001$). (D) Change in mean negative power ($\Delta \bar{P}^-_{ank,total}$) for each condition. (E) Correlation between negative augmentation power and negative total ankle power ($y = 0.047 + 1.3x$, $R^2 = 0.047$, $p = 0.4$).
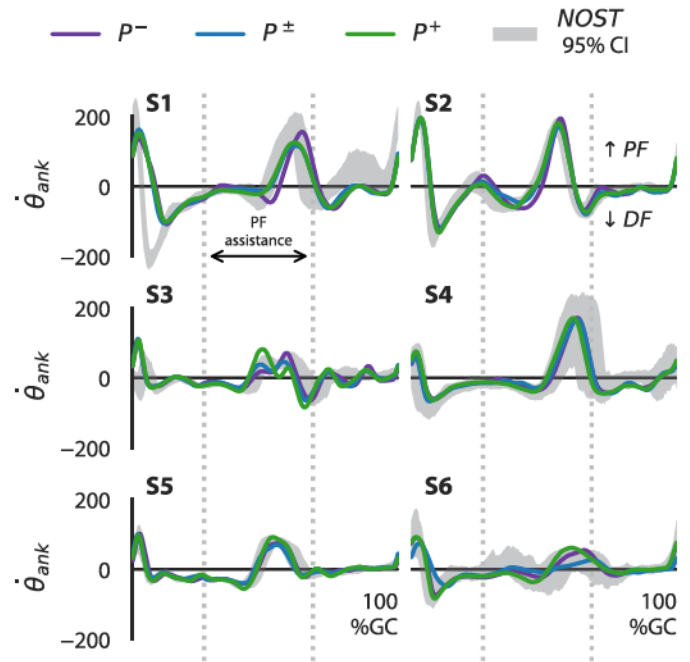


Fig. 8. Comparison of changes in ankle angular velocity ($\dot{\theta}_{ank}$) during PF assistance. Data for *NOST* are an empirical 95% confidence interval.

Fig. 7 shows total ankle power in $P^-$, $P^+$, $P^\pm$, and *NOST* across the entire gait cycle, along with the change in mean positive and negative total ankle power compared to *NOST*. There was a significant correlation between positive augmentation power and positive total ankle power, suggesting that participants were able to utilize augmentation power without lowering their biological ankle's contribution. Though similar phenomena have been shown in healthy individuals [14], prior to the present study it was not yet clear that people poststroke are able to exploit exoskeleton assistance without lowering their own biological contribution. For example, [8] reported no significant differences in paretic ankle work with exoskeleton assistance. Bae *et al.* [21] observed increases in ankle power *symmetry* between the paretic and non-paretic limbs, but did not show specific changes in either limb. The correlation shown in Fig. 7(B) and (C) extends findings from [22], which observed an increase in total ankle power with assistance from a rigid exoskeleton, but did not investigate varying amounts of augmentation power at a constant walking speed.

Opposite to positive power augmentation, there was no significant correlation between negative augmentation power and negative total ankle power (Fig. 7(D) and (E)). This discrepancy suggests that people poststroke utilize negative and positive augmentation power differently. This phenomenon has been suggested in healthy populations [16], but has yet to be observed in people poststroke, who exhibit significant deficits in both negative and positive power production at the ankle. No change in mean total negative ankle power indicates that biological power may have changed, possibly interfering with the Achilles tendon's ability to passively store energy during early stance—in general undesirable. However, there is some speculation that poor muscle coordination in people poststroke

assumption implicit to (7) that ankle kinematics will not change by calculating ankle angular velocity under the three active conditions tested. Using the inverse dynamics estimate of total ankle power (that is, the combined power generated by both the biological ankle and the exosuit), we then evaluated whether augmentation power was actually adding to biological power production.

Fig. 8 shows a comparison of ankle angular velocity during PF assistance among the four conditions tested. Changes in ankle velocity during the region of PF assistance were small, even with substantial differences in assistance torque. There was no significant difference in mean ankle angular velocity over the period of PF assistance across conditions ($p = 0.998$). Specifically, mean RMS difference during the period of PF assistance with respect to *NOST* was $23.08 \pm 16.77°\mathrm{s}^{-1}$ in $P^-$, $18.80 \pm 06.68°\mathrm{s}^{-1}$ in $P^\pm$, and $22.67 \pm 10.90°\mathrm{s}^{-1}$ in $P^+$. Conversely, changes during the period of DF assistance were greater, matching previous work [10], [11] that demonstrated increases in toe clearance.

may inhibit passive energy storage in the Achilles tendon [23]. Notably, repeating the analysis in Fig. 7 using biological negative ankle power revealed only a trend toward decreasing biological power (data not shown).

## VI. Conclusion

To evaluate the effects of PF assistance in people poststroke we used an offline assistance optimization scheme to isolate both positive and negative augmentation power. An experimental evaluation with six participants suggested that offline assistance optimization can be successful despite the assumption that kinematics do not change when assistance is applied. Assistive profiles tuned according to equation (7) delivered either positive or negative augmentation power as desired. Positive augmentation power contributed to total ankle power; negative augmentation power did not. The offline assistance optimization scheme presented here revealed this discrepancy for the first time in clinical populations.

Future work will explore how expressly individualizing $\dot{\theta}_{ank}$ in equation (7) can improve PF assistance in people poststroke. Investigating differences at the muscle level—through techniques such as electromyography or ultrasound—could reveal why people poststroke respond differently to negative and positive augmentation power. Moreover, though the present study examined isolated positive and negative augmentation power, delivering similar amounts of each to the ankle will likely show better clinical outcomes.

## References

[1] E. J. Benjamin *et al.*, "Heart disease and stroke statistics—2019 Update: A report from the American Heart Association," *Circulation*, vol. 139, no. 10, Mar. 2019.

[2] G. E. Gresham, T. E. Fitzpatrick, P. A. Wolf, P. M. McNamara, W. B. Kannel, and T. R. Dawber, "Residual disability in survivors of stroke—the Framingham study," *New England J. Medicine*, vol. 293, no. 19, pp. 954–956, 1975.

[3] S. J. Olney and C. Richards, "Hemiparetic gait following stroke. Part I: Characteristics," *Gait Posture*, vol. 4, no. 2, pp. 136–148, Apr. 1996.

[4] S. Lipfert, M. Gunther, D. Renjewski, and A. Seyfarth, "Impulsive ankle push-off powers leg swing in human walking," *J. Exp. Biol.*, vol. 217, no. 10, pp. 1831–1831, 2014.

[5] J. Leung and A. Moseley, "Impact of ankle-foot orthoses on gait and leg muscle activity in adults with hemiplegia," *Physiotherapy*, vol. 89, no. 1, pp. 39–55, Jan. 2003.

[6] A. Vistamehr, S. A. Kautz, and R. R. Neptune, "The influence of solid ankle-foot-orthoses on forward propulsion and dynamic balance in healthy adults during walking," *Clin. Biomechanics*, vol. 29, no. 5, pp. 583–589, 2014.

[7] J. F. Geboers, M. R. Drost, F. Spaans, H. Kuipers, and H. A. Seelen, "Immediate and long-term effects of ankle-foot orthosis on muscle activity during walking: A randomized study of patients with unilateral foot drop," *Arch. Physical Medicine Rehabil.*, vol. 83, no. 2, pp. 240–245, 2002.

[8] K. Z. Takahashi, M. D. Lewek, and G. S. Sawicki, "A neuromechanics-based powered ankle exoskeleton to assist walking post-stroke: A feasibility study," *J. NeuroEng. Rehabil.*, vol. 12, no. 1, 2015, Art. no. 23.

[9] L. W. Forrester *et al.*, "Clinical application of a modular ankle robot for stroke rehabilitation," *NeuroRehabilitation*, vol. 33, no. 1, pp. 85–97, Jan. 2013.

[10] L. N. Awad *et al.*, "A soft robotic exosuit improves walking in patients after stroke," *Sci. Translational Medicine*, vol. 9, no. 400, Jul. 2017, Art. no. eaai9084.

[11] J. Bae *et al.*, "A lightweight and efficient portable soft exosuit for paretic ankle assistance in walking after stroke," in *Proc. IEEE Int. Conf. Robot. Autom.*, Brisbane, AU, May 2018, pp. 2820–2827.

[12] R. W. Jackson and S. H. Collins, "An experimental comparison of the relative benefits of work and torque assistance in ankle exoskeletons," *J. Appl. Physiol.*, vol. 119, no. 5, pp. 541–557, Sep. 2015.

[13] L. M. Mooney, E. J. Rouse, and H. M. Herr, "Autonomous exoskeleton reduces metabolic cost of human walking during load carriage," *J. Neuro-Eng. Rehabil.*, vol. 11, no. 1, p. 80, 2014.

[14] B. T. Quinlivan *et al.*, "Assistance magnitude versus metabolic cost reductions for a tethered multiarticular soft exosuit," *Sci. Robot.*, vol. 2, no. 2, Jan. 2017, Art. no. eaah4416.

[15] S. H. Collins, M. B. Wiggin, and G. S. Sawicki, "Reducing the energy cost of human walking using an unpowered exoskeleton," *Nature*, vol. 522, no. 7555, pp. 212–215, Apr. 2015.

[16] P. Malcolm *et al.*, "Varying negative work assistance at the ankle with a soft exosuit during loaded walking," *J. NeuroEng.*, vol. 14, no. 1, Dec. 2017, Art. no. 62.

[17] S. Lee, S. Crea, P. Malcolm, I. Galiana, A. Asbeck, and C. Walsh, "Controlling negative and positive power at the ankle with a soft exosuit," in *Proc. IEEE Int. Conf. Robot. Autom.*, Stockholm, May 2016, pp. 3509–3515.

[18] Y. Ding, M. Kim, S. Kuindersma, and C. J. Walsh, "Human-in-the-loop optimization of hip assistance with a soft exosuit during walking," *Sci. Robot.*, vol. 3, no. 15, Feb. 2018, Art. no. eaar5438.

[19] J. Kim *et al.*, "Autonomous and portable soft exosuit for hip extension assistance with online walking and running detection algorithm," in *Proc. IEEE Int. Conf. Robot. Autom.*, Brisbane, Australia, May 2018, pp. 1–8.

[20] G. Lee, Y. Ding, I. G. Bujanda, N. Karavas, Y. M. Zhou, and C. J. Walsh, "Improved assistive profile tracking of soft exosuits for walking and jogging with off-board actuation," in *Proc. IEEE/RSJ Int. Conf. Intell. Robots Syst.*, Sep. 2017, vol. 2017, pp. 1699–1706. [Online]. Available: http://ieeexplore.ieee.org/document/8205981/

[21] J. Bae *et al.*, "Biomechanical mechanisms underlying exosuit-induced improvements in walking economy after stroke," *J. Exp. Biol.*, vol. 221, 2018, Art. no. jeb.168815.

[22] E. M. McCain *et al.*, "Mechanics and energetics of post-stroke walking aided by a powered ankle exoskeleton with speed-adaptive myoelectric control," *J. NeuroEng. Rehabil.*, vol. 16, no. 1, Dec. 2019, Art. no. 57.

[23] G. S. Sawicki, C. L. Lewis, and D. P. Ferris, "It pays to have a spring in your step," *Exercise Sport Sci. Rev.*, vol. 37, no. 3, pp. 130–138, 2009.